geosciences

MDPI

Article

Changes in Land Use and Land Cover Patterns in Two Desert Basins Using Remote Sensing Data

Abdullah F. Alqurashi * and Omar A. Alharbi

Geography Department, Umm Al-Qura University, Makkah 21955, Saudi Arabia; oaoharbi@uqu.edu.sa
* Correspondence: afalqurashi@uqu.edu.sa; Tel.: +966-5999-046-39

Abstract: Land use and land cover (LULC) changes can potentially impact natural ecosystems and are considered key components of global environmental change. The majority of LULC changes are related to human activities. Anthropogenic modifications have resulted in significant changes in the structure and fragmentation of landscapes. This research aimed to analyze LULC changes using satellite images in the following two main basins in the Makkah region: the Wadi Fatimah and Wadi Uranah fluvial systems. First, image classification was conducted using remote sensing data from different satellite platforms, namely the Multispectral Scanner, the Landsat Thematic Mapper, the Enhanced Thematic Mapper Plus, and the Operational Land Imager. Images from these platforms were acquired for the years 1972, 1985, 1990, 2000, 2014, and 2022. A combination of object-based image analysis and a support vector machine classifier was used to produce LULC thematic maps. The obtained results were then used to calculate landscape metrics to quantify landscape patterns and fragmentation. The results showed that the landscape has undergone remarkable changes over the past 46 years. Built-up areas exhibited the most significant increase, while vegetation cover was the most dynamic land cover type. This was attributed mainly to the dry climatic conditions in the study area. These results suggest that LULC changes have influenced the natural environment in the studied area and are likely to contribute to further environmental impacts in the future. Measuring the spatial LULC distribution will help planners and ecologists to develop sustainable management strategies to mitigate future environmental consequences.

Keywords: landscape metrics; land cover pattern; environmental changes; Wadi Fatimah basin; Wadi Uranah basin; Saudi Arabia; change detection

check for updates

Academic Editor: Piotr Migoń

Received: 12 March 2025
Revised: 22 April 2025
Accepted: 13 May 2025
Published: 15 May 2025

Citation: Alqurashi, A.F.; Alharbi, O.A. Changes in Land Use and Land Cover Patterns in Two Desert Basins Using Remote Sensing Data. *Geosciences* **2025**, *15*, 178. https://doi.org/10.3390/geosciences15050178

Copyright: © 2025 by the authors. Licensee MDPI, Basel, Switzerland. This article is an open access article distributed under the terms and conditions of the Creative Commons Attribution (CC BY) license (https://creativecommons.org/licenses/by/4.0/).

1. Introduction

Land use and land cover (LULC) change is considered as one of the most prominent impacts of human activity on the natural environment [1–3]. The ever-increasing population rates and the associated large-scale exploitation of natural resources have caused tremendous and unprecedented modifications to the Earth's surface. One of the principal consequences of population growth is the transformation of natural landscapes into urban areas [4,5], as well as other related activities such as agriculture, industry, and transportation. Understanding LULC change has become necessary to avoid or minimize humans' negative impacts on local natural ecosystems [6].

In recent years, most LULC change information has been obtained from remote sensing data [7]. Remote sensing provides valuable information regarding LULC changes over the last five decades. Using remote sensing data, it is possible to regularly identify, observe, map, and monitor environmental changes across a range of spatial and temporal scales [8].

The accessibility of extensive, systematically collected remote sensing data (e.g., Landsat imagery) has motivated researchers to examine LULC changes using time-series-based methods [9]. Various classification approaches have been developed and used to efficiently derive LULC changes from satellite images, such as deep learning [10], sup-port vector machine (SVM) classification [11,12], and object-based image analysis (OBIA) [13–15]. The integration of SVM classification and OBIA has shown improvements in classification accuracy [16,17]. This integration leverages the advantages of both techniques, where SVM is a superior machine learning methodology with excellent results in pattern recognition [18], while OBIA incorporates contextual information into the classification process [13], effectively improving classification accuracy.

As landscape structure is heterogeneous and dynamic, a quantitative description of LULC change is fundamental to understanding its spatial and temporal patterns and processes [16,19]. Different spatial elements of LULC change—such as patch size, shape, location, distribution, area, arrangement, and connectivity—can serve as key variables for quantifying LULC patterns and processes [20]. A variety of landscape metrics have been developed to quantify landscape patterns at different scales [21–23]. Information extracted from landscape metrics provides valuable insights into the spatial arrangements of different land cover classes [24]. Such information can greatly support planning efforts and environmental assessments, particularly for fast-growing nations such as Saudi Arabia.

Saudi Arabia frequently experiences various environmental changes due to its extreme climate, including drought, water scarcity, and wind erosion [25]. Human-induced LULC changes occur more rapidly than natural changes, placing greater stress on this fragile environment [26,27]. In the 1970s, the government launched a nationwide development program funded by substantial oil revenues [26,28]. This development has led to significant changes in various environmental components, including hydrological processes, climate systems, landscape ecology, and land cover patterns. Given the rapid and dynamic nature of LULC changes, an automated method for identifying these changes is essential for analyzing their spatial and temporal patterns, as well as their distribution. This information can assist planners and ecologists in formulating effective and sustainable management strategies to mitigate future environmental impacts.

Makkah Province is the third-largest area in Saudi Arabia and the second-most populous region, with a population of 8,021,463, according to the 2022 population census (General Authority of Statistics, 2022). The province is home to Makkah city, the most revered holy site for Muslims worldwide. Each year, millions of Muslims visit the city to perform the Hajj pilgrimage, with over three million national and international pilgrims gathering simultaneously during the Hajj season. Beyond Hajj, millions travel to Makkah throughout the year to perform Umrah, with the number of visitors expected to rise to 15 million in the coming years, in line with Saudi Vision 2030. The substantial influx of pilgrims during Hajj presents various challenges for Makkah city, including housing, transportation, and the provision of basic services [29]. This influx exacerbates existing urban challenges [30]. Along with local population growth, the increasing number of visiting pilgrims has led to extensive land modifications and significant changes in LULC over the past five decades.

A number of studies have emphasized the impact of LULC changes, as well as urban expansion, in this region. For instance, Alqurashi and Kumar [26] used Landsat images from 1986 to 2013 to detect LULC changes in Makkah and Al-Taif and concluded that LULC had changed over the last 30 years in both cities. Alqurashi and Kumar [31] analyzed Landsat data from 1985 to 2014 in three Saudi Arabian cities, including Makkah, and found that urban expansion had modified land use in all three cities. Jelil Niang et al. [32] monitored LULC changes in Al-Aziziyah, Makkah, between 1967 and 2005 using CORONA

and QuickBird images and concluded that urban expansion had occurred at the expense of initial geomorphic forms, such as alluvial plains, isolated hills, extended mountain ridges, and mountain masses. Alqurashi [33] quantified the spatiotemporal urban growth patterns in three Saudi Arabian cities, including Makkah, and found that the city had experienced significant urban growth over the past few decades. However, most previous studies have only measured the extent and type of LULC changes in the region. Information regarding the interactions between different land cover types and changes in landscape patterns over time is essential for understanding the causes and consequences of spatial heterogeneity.

This research, therefore, aims to analyze LULC changes using multi-temporal remote sensing data and landscape metrics to quantify the land cover patterns in the following two major basins in Makkah: the Wadi Fatimah and Wadi Uranah basins. The objectives of this research are as follows: (1) to conduct LULC classification on six satellite images acquired in 1972, 1985, 1990, 2000, 2014, and 2022 using an integrated approach combining OBIA and SVM classification for the selected landscapes and (2) to analyze the spatiotemporal patterns of LULC changes using landscape metrics. The results of this study will provide an overview of the impacts of LULC changes to help local planners and decision makers assess past patterns and manage expected LULC changes in the future.

2. Study Area

The study area comprises the following two major upstream basins of fluvial systems in Makkah Province: the Wadi Fatimah and Wadi Uranah fluvial systems (Figure 1). The landscape includes the holy city of Makkah and the western part of Al-Taif city, including the Al-Hada district. Makkah, the holiest city in Islam, is located near the study area in the western part of the region. Al-Taif is considered as the most important tourist city in Saudi Arabia. The region is one of the most urbanized and populated areas in the province.

According to the General Authority of Statistics, Makkah had a population of 2,427,924 in 2022, while Al-Taif had a population of 913,374 in the same year. The region also contains some agricultural land, with most of the arable land being spread across Wadi Fatimah in the north and Wadi Uranah in the south. The eastern part of the study area (mountainous region) receives a considerable amount of rainfall, averaging more than 220 mm per year, while the western part receives less than 100 mm per year [34].

The development of Saudi Arabian cities has progressed through three main phases. The first phase occurred during the 1970s, when the government utilized oil revenues to support national development, leading to a significant increase in built-up areas across many regions [35]. The second phase began in the late 1990s and was characterized by development aimed at enhancing economic growth [36]. The third phase started in 2016 with the launch of Saudi Vision 2030, which marked a strategic shift toward economic diversification. During the first and second phases, the government promoted urban expansion through interest-free loans, which contributed to rapid and widespread growth [35]. In the third phase, the focus has shifted toward investment, tourism, and industrial development as key drivers of economic progress. These initiatives have the potential to significantly influence LULC changes in the Wadi Fatimah and Wadi Uranah basins. The purpose of this study is to assess the LULC changes that occurred during these three phases.

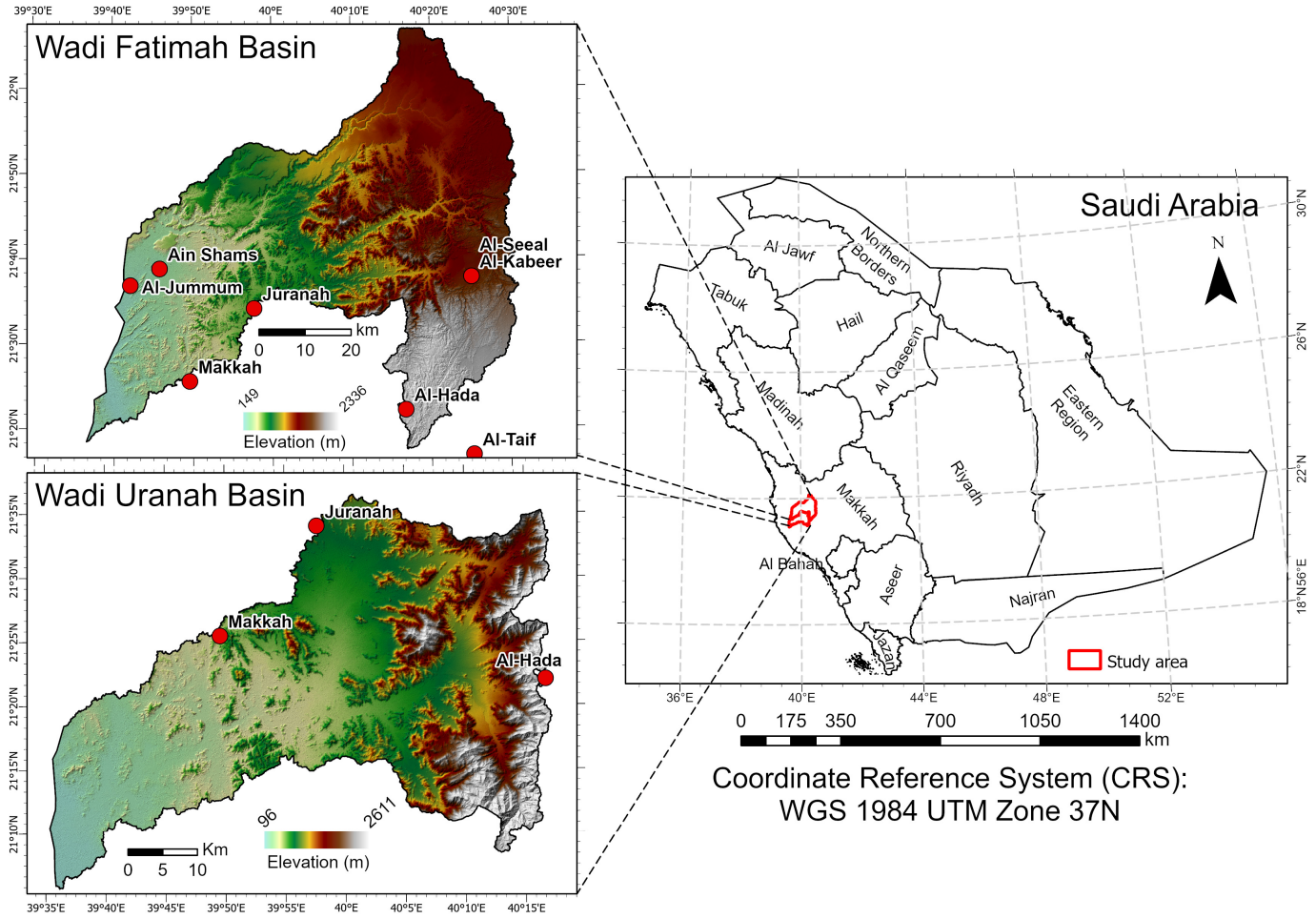


Figure 1. The location of the study areas in Saudi Arabia.

3. Materials and Methods

3.1. Data and Pre-Processing

The primary data used in this research were acquired from the following four satellite platforms: the Multispectral Scanner (MSS), the Thematic Mapper (TM), the Enhanced Thematic Mapper Plus (ETM+), and the Operational Land Imager (OLI). Six images, acquired in 1972, 1985, 1990, 2000, 2014, and 2022, were downloaded from the US Geological Survey data warehouse via the GloVis site (Table 1). All images used in this study had a spatial resolution of 30 m, except for the 1972 MSS image, which was resampled from a 60 m pixel size to 30 m to ensure a consistent spatial resolution across all datasets using the cubic convolution (CC) technique [37]. All images were georeferenced as Level-1 products. The required pre-processing tasks were performed for all images using ENVI 5.3 software (Figure 2). Bands 1 to 4 in MSS, 1 to 5 and 7 in TM and ETM+, and 1 to 7 in OLI were used in the classification process. The selected images were acquired during the summer months (July, August, and September), except for the 1985 image, which was acquired in spring (March). Although selecting images from the same season is important for change detection to minimize the effects of seasonal variation, the only available images for the 1985 period in the study area were from winter and spring. Therefore, the spring image was selected for 1985 in this research.

Table 1. Information on Landsat data used for LULC classification.

No.	Sensor	Path/Row	Date	Grid Cell Size (m)	No. of Bands [1]
1	MSS	182/45	10 September 1972	60	4
2	TM	169/45	30 March 1985	30	6
3	TM	169/45	27 August 1990	30	6
4	ETM+	169/45	6 August 2000	30	6
5	OLI	169/45	5 August 2014	30	7
6	OLI	169/45	15 July 2022	30	7

[1] Number of bands used in the classification process.

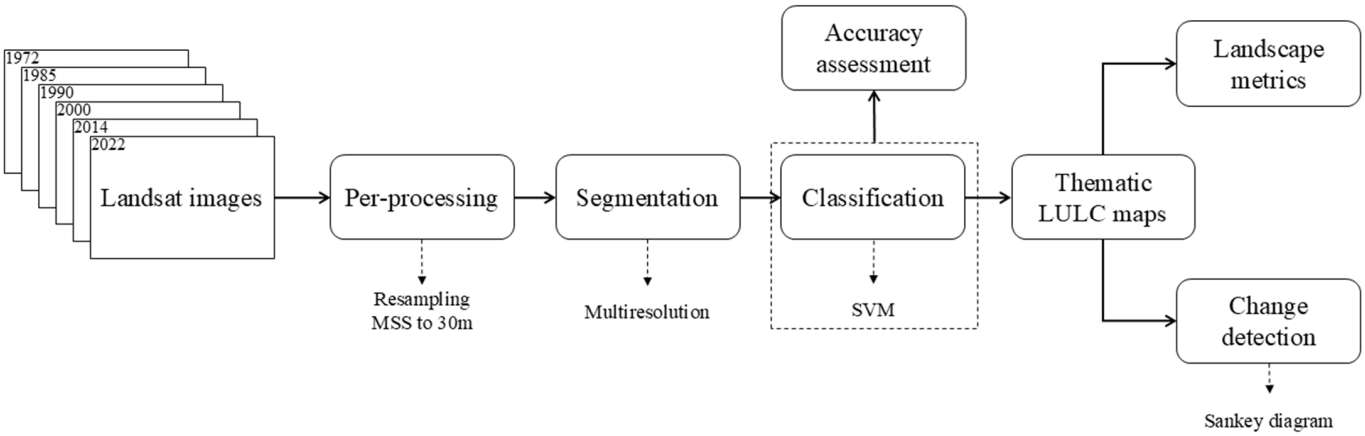


Figure 2. Flowchart of the research methodology.

3.2. Segmentation and Classification

The classification analysis of the Landsat images was conducted using OBIA. Both image segmentation and classification were involved in the OBIA process (Figure 2). The procedure started with image segmentation, where the remotely sensed image was partitioned into distinct objects based on various factors, including texture, color, spatial, and spectral properties [38,39]. To define the LULC classes, a multi-resolution segmentation algorithm was employed. This approach followed a bottom-up region-merging process, in which similar pixels were progressively grouped into larger objects according to a defined scale factor and a heterogeneity criterion [40]. The scale parameter setting was 5, with shape and compactness settings of 0.1 and 0.8, respectively.

The segmented images were then classified using SVM classification (Figure 2). Recently, SVM classification has been widely used among various remote sensing classification algorithms in multiple applications (e.g., [41–43]). SVM is a non-parametric, supervised machine learning method that utilizes a training algorithm to identify an optimal hyperplane, effectively partitioning datasets into a predefined set of distinct classes [44]. SVM is essentially a linear binary classifier that assigns a given test sample to one of two possible classes [44].

There are two key advantages of using the SVM algorithm instead of traditional image classification algorithms. First, SVM has a strong generalization capability, reducing the risk of overfitting and over-smoothing [45]. This is achieved when the kernel width parameter is appropriately sized [44]. Second, SVM can achieve a higher classification accuracy even with small training datasets [46].

In this research, training datasets were initially created for all land cover classes. The following give land cover classes were identified in the study area: bare soil, built-up areas,

rocky land, vegetation cover, and water. Each image was classified separately using a linear kernel function, with the regularization parameter (C) set to 2.

3.3. Accuracy Assessment Analysis

The accuracy of image classification was tested using a stratified random sampling approach to generate reference points. Reference sample points were created for each classified image using the Landsat raw image for each specific date for the 1972, 1985, 1990, 2000, and 2014 images. Google Earth images were used to create reference sample points for the 2022 image. The reference points were generated separately for each basin. Since the extent of the Wadi Fatimah basin is larger than that of the Wadi Uranah basin, the number of sample points varied between them.

For the Wadi Fatimah basin, 880, 1050, 1130, 1320, 1560, and 1620 sample points were created for the years 1972, 1985, 1990, 2000, 2014, and 2022, respectively. Similarly, for the Wadi Uranah basin, 710, 960, 1030, 1160, 1340, and 1430 sample points were identified for the same years. The classification of each image was compared to the reference points, and a confusion matrix was computed to calculate overall accuracy and the kappa coefficient, as well as the user's and producer's accuracies.

3.4. Landscape Metrics

Landscape metrics were calculated using the LecoS (Landscape ecology Statistics) tool, an open-source plugin integrated into QGIS processing software [46]. The computation of landscape metrics was carried out at both the class and landscape levels.

At the class level, the following five indices were calculated: the number of patches (NP), patch density (PD), landscape proportion (LP), class area (CA), and the largest patch index (LPI). At the landscape level, the following three metrics were computed: Shannon's diversity index (SHDI), Shannon's evenness index (SHEI), and Simpson's diversity index (SIDI) for 1972, 1985, 1990, 2000, 2014, and 2022. These metrics were selected to analyze the patterns of LULC changes. They have proven to be effective tools for investigating the degree of landscape fragmentation associated with urban expansion and LULC changes in several previous studies [19,47–50]. Table 2 provides information on the type and description of each metric used, based on McGarigal et al. [51].

Table 2. List of landscape metrics used in this research.

Name and Level	Type	Equation	Description *
Number of patches (NP) (class)	Area		Quantifies the NPs for each individual class
Patch density (PD) (class)	Aggregation	$PD = \frac{NP}{A}(10,000)(100)$ A is the total area (m^2)	Describes the landscape fragmentation
Landscape proportion (LP) (class)	Area	$LP = \frac{\sum_{j=1}^{n} c^{ij}}{A}$ c^{ij} is the class area	Represents the class size of the total land cover classes (cells)
Class area (CA) (class)	Area	$CA = Sum(c^{ij})$	Measures the landscape composition of a particular patch type
Largest patch index (LPI) (class)	Area	$LPI = \frac{\sum_{j=1}^{n} a^{ij}}{A}$ a^{ij} is the area of the patch	Quantifies the percentage of total landscape area comprised by the largest patch
Shannon's diversity index (SHDI; landscape)	Heterogeneity	$SHDI = -\sum_{i=1}^{m} P_i \ln P_i$ P_i is the class proportion	Based on information theory and representing the amount of information per patch

Table 2. *Cont.*

Name and Level	Type	Equation	Description *
Shannon's evenness index (SHEI; landscape)	Heterogeneity	$SHEI = -\frac{\sum_{i=1}^{m} P_i \ln P_i}{\ln m}$ m is the number of classes	Measures the distribution of area among patch types
Simpson's diversity index (SIDI; landscape)	Heterogeneity	$SIDI = 1 - \sum_{i=1}^{m} {P_i}^2$	The probability that any two patches drawn at random will represent different patch types

* The descriptions of the metrics were adopted from McGarigal, Cushman, Neel, and Ene [45].

4. Results

4.1. Accuracy Assessment

The overall accuracies (OAs), kappa coefficient, and user's and producer's accuracies showed satisfactory results for the classified images in both study areas, indicating that the number of correctly classified pixels corresponded to the correct category (Table 3). However, the water class exhibited a low producer's accuracy (PA) for the 2000 classified image in the Wadi Uranah basin and a low user's accuracy (UA) in the Wadi Fatimah basin for the same period. This may be attributed to intermixing between water and other land cover types in the 2000 classified images.

Table 3. Accuracy assessment of the classified images.

Wadi Fatimah basin												
	1972		1985		1990		2000		2014		2022	
Class	PA	UA	PA	UA	PA	UA	PA	UA	PA	UA	PA	UA
Rocky	96.4	98	96.9	99.7	98.5	99.2	96.4	99.5	98	99.6	100	100
Bare soil	93.5	88.9	99.1	89.9	96.7	95.2	97.7	88.3	98.4	93.3	100	95
Vegetation	100	100	100	100	100	100	100	100	100	100	100	100
Built-up	100	100	93.3	100	100	95.2	83.3	96.1	100	100	100	100
Water	0	0	0	0	0	0	100	62.5	100	100	100	100
OA	95.8		97.3		98.1		96.1		98.2		98.7	
Kappa	0.89		0.94		0.95		0.91		0.95		0.97	
Wadi Uranah basin												
	1972		1985		1990		2000		2014		2022	
Class	PA	UA	PA	UA	PA	UA	PA	UA	PA	UA	PA	UA
Rocky	100	93.5	98.2	98.2	95.7	98.5	94.5	93.8	93.3	93.3	95.1	94.1
Bare soil	94.7	98.9	99.1	94.1	98.5	96.3	93	92.3	90.5	82.5	93.2	95
Vegetation	100	100	100	100	100	100	80	80	100	100	94.1	100
Built-up	87.5	100	95	100	100	39.3	100	95.4	96.6	91.8	97	95.5
Water	0	0	72.2	100	0	0	66.7	100	100	100	100	93.3
OA	96.7		96.6		97.2		93.2		93.05		94.8	
Kappa	0.94		0.95		0.95		0.89		0.89		0.92	

4.2. LULC Changes (1972–2022)

LULC changed considerably between 1972 and 2022 in both basins (Figures 3 and 4). In this context, the urban built-up area expanded from the urban core in multiple directions in the study areas. The built-up area was essentially clustered around the city center of Makkah in 1972; however, it expanded in clear directions (north, east, and southeast) between 1972 and 1985 (Figure 4). The spatial urban expansion in these directions is strongly related to the primary highways connecting Makkah to other major cities, such as Jeddah in the west, Al-Taif and Riyadh in the east and south, and Madinah in the north.

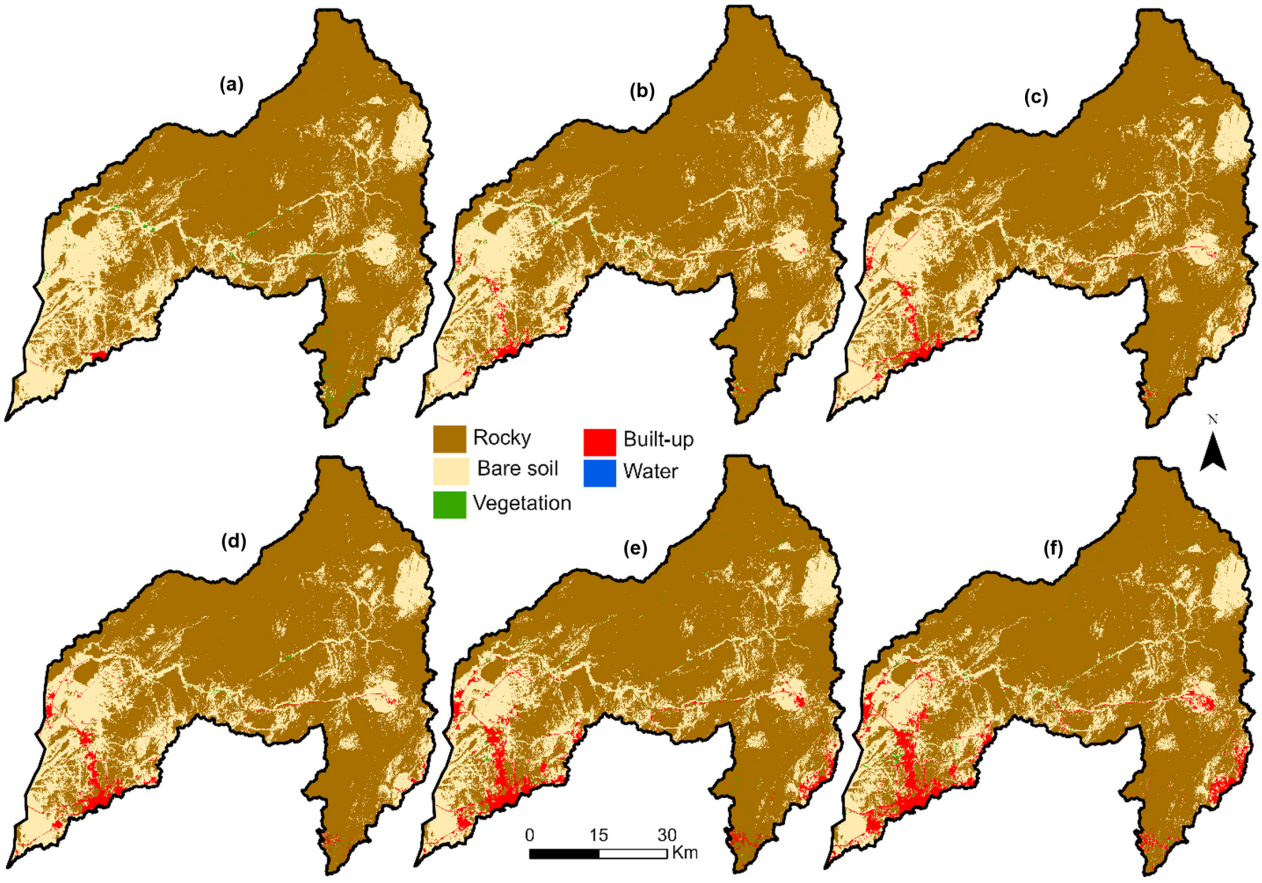


Figure 3. LULC classification maps for (**a**) 1972, (**b**) 1985, (**c**) 1990, (**d**) 2000, (**e**) 2014, and (**f**) 2022 in the Wadi Fatimah basin.

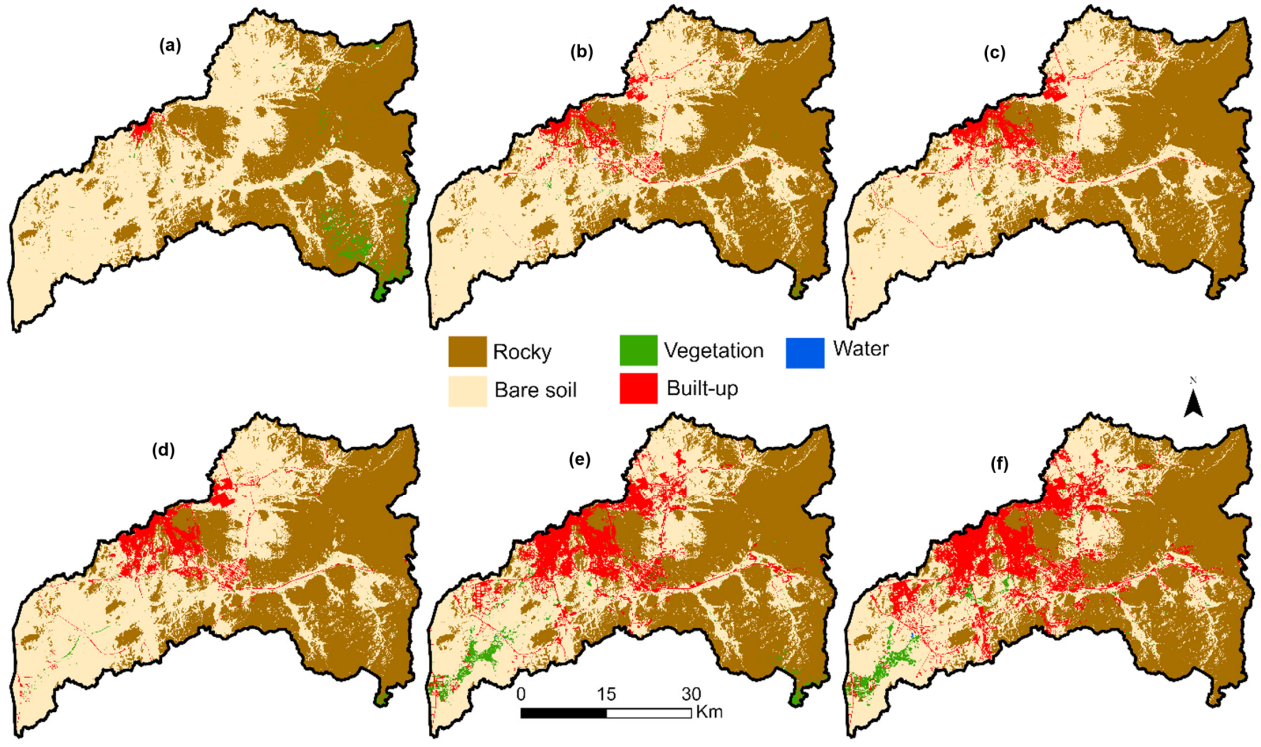


Figure 4. LULC classification maps for (**a**) 1972, (**b**) 1985, (**c**) 1990, (**d**) 2000, (**e**) 2014, and (**f**) 2022 in the Wadi Uranah basin.

The urban expansion between 1985 and 1990 through to 2000 did not show extra expansion in new directions; however, the urban expansion stripes in the east, north, and southeast showed denser and wider urban patterns than those of the 1972–2022 time period. Unlike the pattern and density of urban expansion between 1990 and 2000, spatial urban expansion was massive and extensive between 2014 and 2022. It occurred in all directions in a radial pattern and was highly dense as well. This could be attributed to the remarkable increase in the country's national budget in response to the rise in oil prices between 2005 and 2014 [13]. This expansion of the national economy during that time allowed the government to orient development toward major cities such as Makkah.

4.3. LULC Change Patterns (1972–2022)

LP represents the proportion of each land cover type within the Wadi Fatimah and Wadi Uranah landscapes (Figure 5a). The trend of built-up areas showed an overall increase in urban development, though the rate of expansion varied over time. Nevertheless, the LP of built-up areas in the Wadi Uranah basin indicated more expansion than that in the Wadi Fatimah basin.

The NP of vegetation cover showed an increasing pattern between 1972 and 2014 in both basins (Figure 5b). This increase indicates greater fragmentation and dispersion over time. Similarly, the NP of built-up areas significantly increased, reflecting increased complexity in the study area after 1972. In other words, in 1972, the built-up area was coherent and clustered in a small pattern. However, after 1972, expansion led to fragmentation into several patches, accompanied by increased patch isolation. This trend was clearly visible in 2014 and 2022. The PD of vegetation cover was highest in 2014 in both basins. However, the PD value of vegetation cover in Wadi Uranah was higher than that in Wadi Fatimah (Figure 5c).

The increase in built-up area was limited and gradual between 1972 and 2000 (Table 4). However, after 2000, the built-up area expanded significantly. In 1972, the built-up area covered 881.73 ha and 1104.03 ha in Wadi Fatimah and Wadi Uranah, respectively. By 2000, the absolute area of built-up land had increased to 8272.17 ha and 12,503.52 ha, with total differences of approximately 7390 ha and 11,399 ha, respectively. The difference in the absolute built-up area exceeded 18,300 ha between 2000 and 2014.

Table 4. Class area (CA) for each land cover type (in ha) for 1972, 1985, 1990, 2000, 2014, and 2022.

Wadi Fatimah basin						
Class	**1972**	**1985**	**1990**	**2000**	**2014**	**2022**
Bare soil	108,025.38	105,259.95	103,562.91	101,680.29	94,440.42	91,405.71
Rocky	303,099.02	302,481.06	302,385.12	304,877.25	302,565.15	302,085.23
Built-up	881.73	3865.77	6163.65	8272.17	16,245.27	21,111.03
Vegetation	2607.57	1006.92	502.11	777.96	2362.05	2397.06
Water	0	0	0	6.21	1.35	14.22
Wadi Uranah basin						
Class	**1972**	**1985**	**1990**	**2000**	**2014**	**2022**
Bare soil	108,523.44	103,290.57	101,169.36	98,544.42	84,494.25	77,826.96
Rocky	106,691.8	106,007.67	105,953.22	105,375.06	103,081.14	101,846.79
Built-up	1104.03	7014.15	9737.82	12,503.52	24,775.56	33,131.25
Vegetation	4718.61	712.98	177.48	612.54	4669.2	4165.83
Water	0	12.51	0	2.52	18	30.6

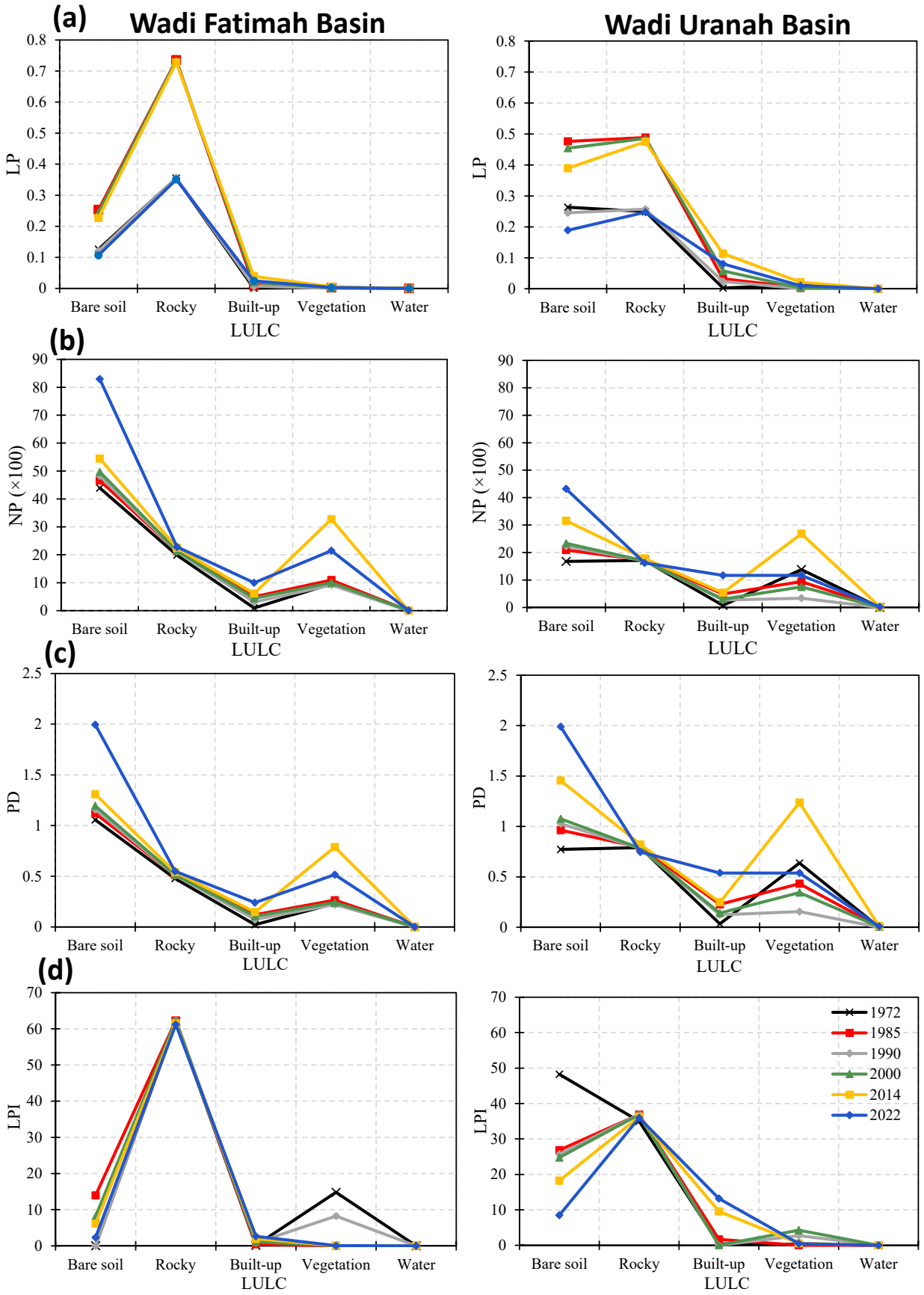


Figure 5. Landscape proportion (LP) (**a**), number of patches (NP) (**b**), patch density (PD) (**c**), and largest patch index (LPI) (**d**) changes between 1972 and 2022 in Wadi Fatimah basin and Wadi Uranah basin.

These results suggest that urban development in the study area can be categorized into the following two main phases: the first occurring after 1972 and the second after 2000. While urban development in the first phase was slow and gradual, it was rapid and extensive in the second phase. However, the built-up area in the Wadi Uranah basin showed a remarkable increase between 1972 and 1985.

Vegetation cover also increased in 2014 and 2022 by approximately 7000 ha, indicating growth in green spaces or agricultural lands in the studied landscape. Most water surfaces in the study area dry out throughout the year due to rising temperatures and evaporation [36].

The SHDI showed an increase over time between 1972 and 2022 in both basins, indicating that LULC changes influenced both study areas (Figure 6a). The differences in the initial SHDI values in 1972 highlight variations in the starting landscape conditions. Later, urban expansion balanced the changes in LULC across both study areas. However, the Wadi Uranah basin exhibited greater diversity than the Wadi Fatimah basin.

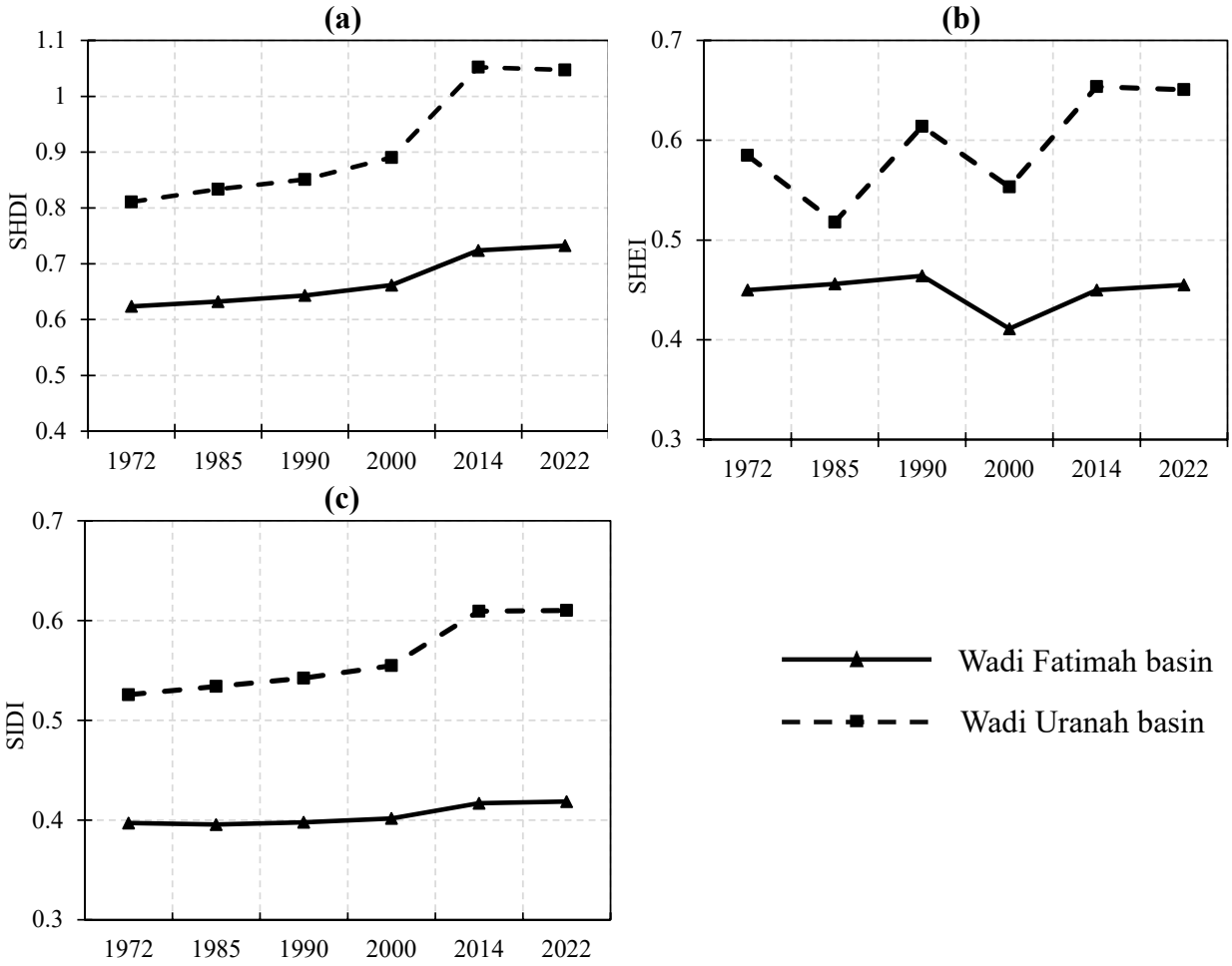


Figure 6. Shannon's Diversity Index (SHDI) (**a**), Shannon's Evenness Index (SHEI) (**b**), and Simpson's Diversity Index (SIDI) (**c**) between 1972 and 2022 in the Wadi Fatimah basin and Wadi Uranah basin.

The SHEI values for the Wadi Fatimah basin ranged from 0.41 to 0.46 over the period from 1972 to 2022 (Figure 6b). These values suggest a relatively stable evenness in the distribution of land cover types within the Wadi Fatimah basin throughout the study period. The fluctuations between 0.41 and 0.46 indicate minor variations in evenness but, overall, no significant change in the relative abundance of different ecosystem components. In contrast, the SHEI values for the Wadi Uranah basin showed more variation, ranging from 0.51 to 0.65 over the same period (Figure 6b). The increasing trend from 0.51 in 1972 to 0.65

in 2022 suggests a gradual improvement in the evenness of land cover types within the Wadi Uranah basin over time.

The SIDI values showed differences between the Wadi Fatimah and Wadi Uranah basins. While the landscape of the Wadi Fatimah basin indicated relatively stable diversity and dominance patterns, the Wadi Uranah basin exhibited a gradual increase in diversity and a decrease in dominance over time (Figure 6c).

4.4. Change Detection

The built-up area expanded more in the Wadi Uranah basin than in the Wadi Fatimah basin (Figures 7 and 8). In the Wadi Uranah basin, most of the land converted to built-up areas was previously bare soil. The increase in built-up areas nearly doubled between 2000 and 2014 (Figure 8). A significant increase was also observed in the Wadi Fatimah basin during the same period (Figure 7). However, the number of built-up areas between 2014 and 2022 was lower than that in the Wadi Uranah basin. Other land cover features, such as vegetation and water, showed inconsistent changes between 1972 and 2022. Vegetation cover decreased between 1972 and 2000, but increased again during the 2014–2022 period (Figure 8).

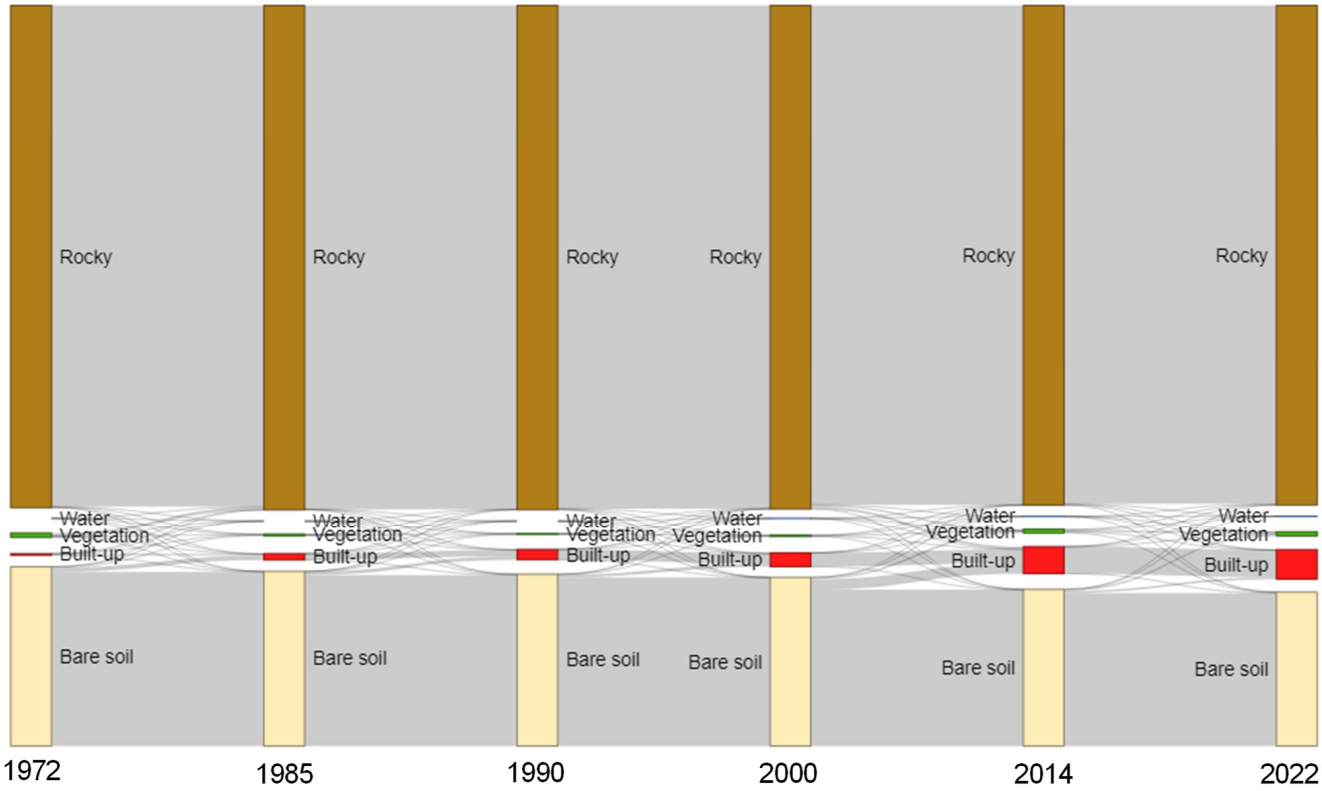


Figure 7. Land use and land cover changes between 1972 and 2022 in the Wadi Fatimah basin.

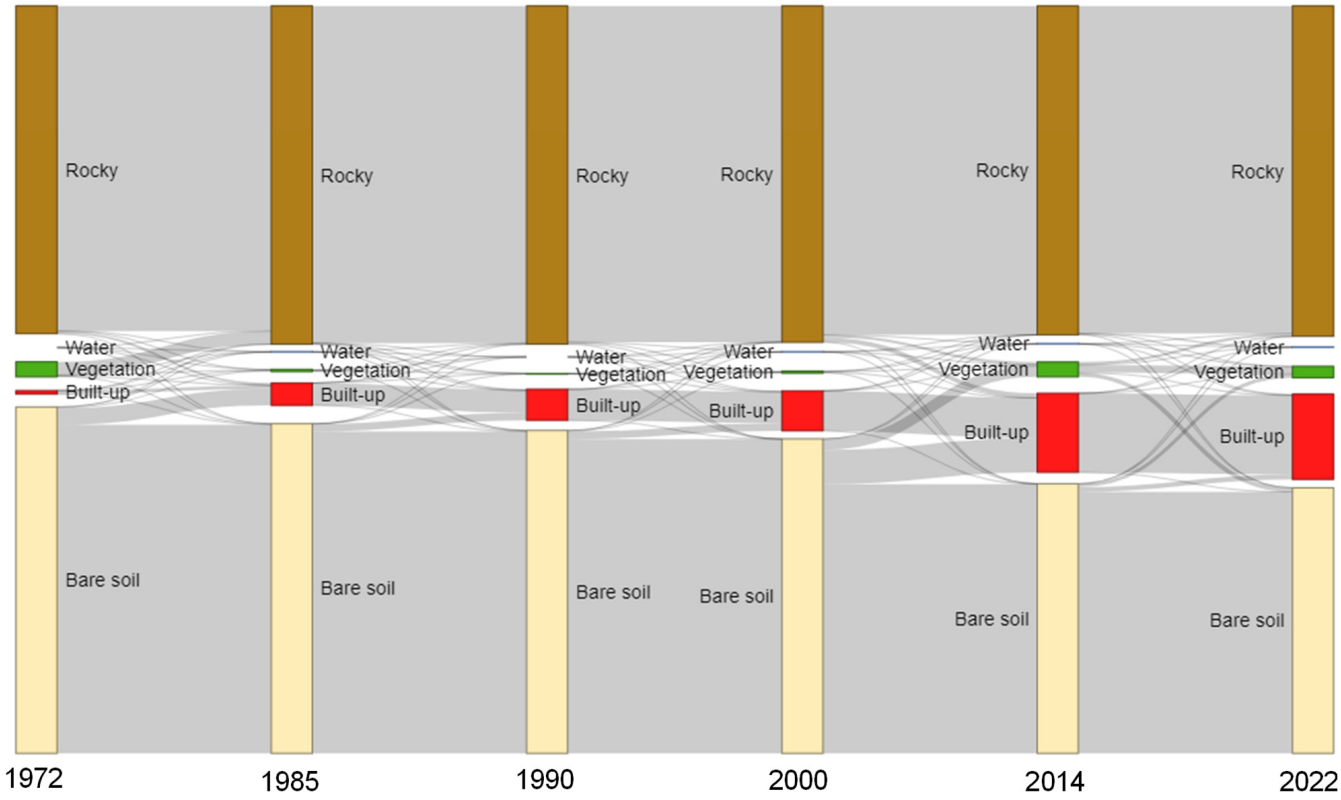


Figure 8. Land use and land cover changes between 1972 and 2022 in the Wadi Uranah basin.

5. Discussion

5.1. Urban Expansion (1972–2022)

The results indicate that urban development was faster in the Wadi Uranah basin than in the Wadi Fatimah basin. The built-up area was about 900 hectares in 1972 in Wadi Fatimah, whereas it was 1100 hectares during the same period in Wadi Uranah. The built-up area had nearly doubled by 1985 in the Wadi Uranah basin and continued to increase until 2022, growing at a faster rate than in the Wadi Fatimah basin. The development size may be attributed to the land structure of both basins. The complex topographic structure of Wadi Fatimah may have significantly restricted urban development. This can be explained by the total area of rocky land in Wadi Fatimah, which exceeds 300,000 hectares. In contrast, the Wadi Uranah basin had unoccupied land without a heavy topographic structure. This could have encouraged housing agencies to build new constructions in flat areas, where construction costs would be lower than those in areas with complex topography. The impact of elevation on urban development has been reported in several studies [36,52,53].

Changes in urban growth over the 50-year period also varied. While the early stage of development showed reasonable expansion between 1972 and 1985, most urban expansion occurred between 2000 and 2014 in both basins (Figure 9). The size of urban growth during the later 14-year period (2000–2014) was greater than that during the earlier 28-year period (1972–2000). Such a massive increase is mainly attributed to government policy. The increase in oil revenues resulted in a rise in national budgets, which, in turn, was used to support large-scale housing development in Saudi Arabia. Housing construction was funded by the government through no-interest loans [28]. This policy was introduced at that time to support the development process and reduce housing shortages [35]. The 2014–2022 period witnessed large expansion in both basins, suggesting that urban growth will continue at a similar rate in the near future.

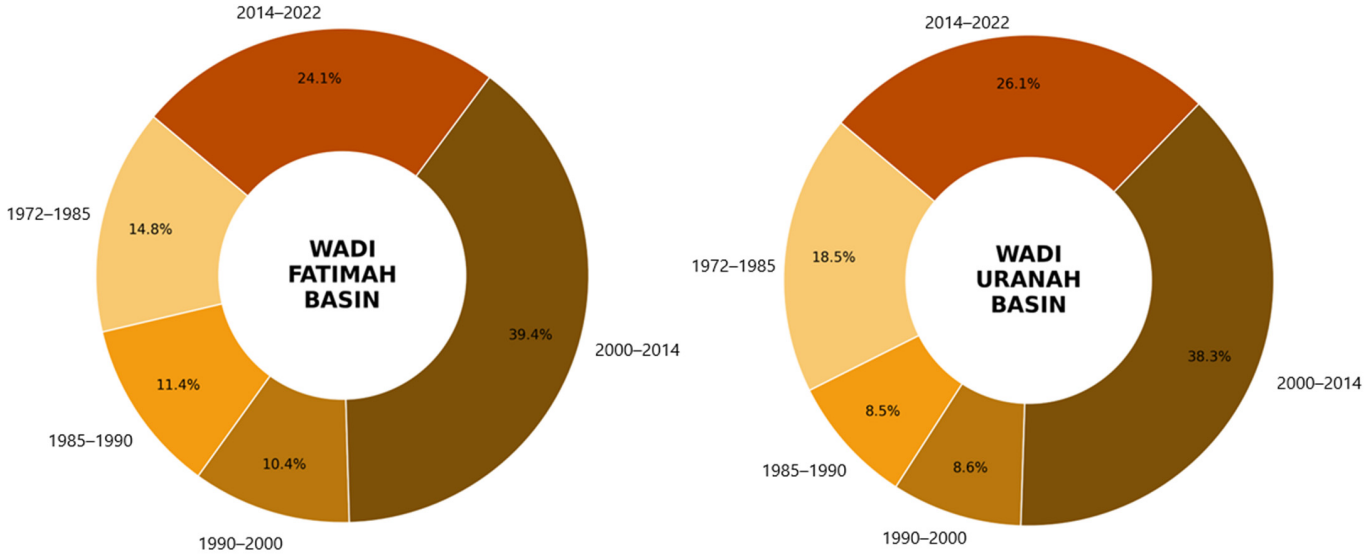


Figure 9. The size of urban growth in Wadi Fatimah basin and Wadi Uranah basin during each time interval.

5.2. LULC Patterns

Urban cover in both basins exhibited a fragmented spatial pattern. However, landscape metrics revealed that urban growth in the Wadi Uranah basin was more fragmented compared to the Wadi Fatimah basin. This is primarily attributed to the concentration of Makkah's urban expansion within the Wadi Uranah basin between 1985 and 2022. The basin encompasses the majority of Makkah's holy sites, including Mina, Muzdalifah, and Arafat, which are central to the Hajj pilgrimage and host most of its rituals and events. As these areas are designated as public property and private ownership is prohibited, the government has developed extensive infrastructure and facilities to support Hajj activities. In recent years, the number and scale of these structures—such as buildings, permanent tents, and parking lots—have expanded substantially to accommodate the increasing number of visiting pilgrims. Thousands of square kilometers are now covered by such facilities across Mina, Muzdalifah, and Arafat. While these facilities remain largely unoccupied throughout the year, except during the Hajj season, their extensive spatial footprint has significantly contributed to the expansion of the built-up areas [30]. Furthermore, the structural layout of these facilities, often separated and specialized in function, has resulted in a more fragmented urban landscape. This pattern of development highlights the need for strategic planning to manage future urban growth while minimizing adverse impacts on the natural environment.

Urban expansion is influenced by various driving factors, including infrastructure development. Several studies have highlighted the significant role of public infrastructure—particularly road networks—in shaping urban development across different regions of Saudi Arabia. For instance, Alqurashi, Kumar, and Al-Ghamdi [36] concluded that accessibility to urban facilities, services, and security contributes to increased construction and urban expansion near major roads in Saudi cities. Similarly, Bindajam and Mallick [54] emphasized that road network connectivity has been a key driver of urban growth in Abha, Saudi Arabia. In the case of the Wadi Fatimah and Wadi Uranah basins, urban expansion over the past five decades appears to be closely associated with the development and extension of road networks.

The results also indicate that vegetation cover fluctuated over time in both the Wadi Fatimah and Wadi Uranah basins. While vegetation biomass was relatively high in 1972, it declined significantly in the subsequent years—1985, 1990, and 2000. In more recent years

(2014 and 2022), vegetation cover has shown a notable increase. These fluctuations are likely influenced by climatic variability in both basins. As part of an arid environment, most vegetation communities consist of xeromorphic dwarf shrublands [25], which typically emerge following rainstorms and disappear shortly thereafter due to high temperatures and intense evaporation. Larger trees and shrubs are generally confined to valley (wadi) floors [25]; however, even these communities are often sparsely distributed due to limited water availability, harsh climatic conditions, and poor soil nutrient content [55]. Our findings also revealed that vegetation cover in both Wadi Fatimah and Wadi Uranah has become increasingly fragmented over time. This is supported by the observed increase in the NP of vegetation cover between 1972 and 2022, indicating a more dispersed and fragmented spatial pattern.

Similar to vegetation cover, water availability also fluctuated between 1972 and 2022 in both basins. Wadi Fatimah had virtually no water presence until 2000, with a modest increase observed in 2022 (14.22 ha). In contrast, Wadi Uranah consistently exhibited a greater extent of water bodies. Nevertheless, water resources remain extremely limited in both basins, reflecting the arid climatic conditions. In desert regions, water bodies are primarily fed by rainfall, which is scarce. Due to high temperatures and intense evaporation, most of these water bodies dry up throughout the year [36]. This also applies to drainage systems, which, in Saudi Arabia, are typically ephemeral—they remain dry most of the year and only carry water following heavy rainfall events.

The analysis of landscape metrics revealed that both the Wadi Fatimah and Wadi Uranah basins exhibited increasingly complex patterns in most land cover types. This is particularly evident in the increase in the NP for built-up areas after 1972, indicating that urban development was initially compact and concentrated in small, coherent clusters. Over time, however, built-up areas became more fragmented, forming multiple dispersed patches. A similar fragmentation trend was observed in vegetation cover, which appeared as scattered and isolated patches throughout both basins. This growing landscape complexity presents significant ecological challenges, potentially affecting habitat connectivity, biodiversity, and ecosystem stability in the region.

5.3. LULC Changes Implications

LULC changes have significant impacts on various ecological and hydrological components, including surface runoff, vegetation cover, soil properties, and water flow dynamics, primarily through alterations in surface roughness [56–58]. These transformations are reshaping Earth's ecosystems and contributing to the intensification of climate change [59,60]. Our results indicate that both the Wadi Fatimah and Wadi Uranah basins have experienced substantial LULC changes over the past five decades. These changes have been largely driven by the rapid expansion of urban areas, which has occurred in all directions across both basins. Uncontrolled urban growth poses serious challenges for planners and environmentalists in Saudi Arabia, particularly in regions already facing natural constraints due to the harsh desert environment.

As a desert region, much of Saudi Arabia's land is naturally sensitive to change due to its fragile ecosystems, low resilience, and extreme climate conditions. Urban expansion and land use changes accelerate environmental damage through habitat destruction, resource depletion, pollution, climate alteration, and changes in water resources [61] and landforms. Both the Wadi Fatimah and Wadi Uranah basins are unique and ecologically significant compared to the surrounding harsh, arid areas. These systems play a crucial role in the desert ecosystem by supporting vegetation cover, wildlife, and human settlements. Uncontrolled urban expansion can disrupt their natural balance, leading to increased

environmental degradation [62]. Sustainable land management practices are essential to ensure the long-term health of these fragile ecosystems.

LULC changes are expected to intensify in the future as a result of continued urban expansion. The findings of this research show that, in 1972, urban areas were primarily concentrated near the urban core. However, significant urban growth occurred during the 1980s and continued in the subsequent decades. A similar pattern of expansion is likely to continue in both basins. This ongoing urban growth is expected to further reduce other land cover types in the region and place additional stress on the already fragile arid environment. Therefore, effective urban planning is essential to manage current development and mitigate the future impacts of LULC changes in the Wadi Fatimah and Wadi Uranah basins.

5.4. Ecological Planning Implementations

Monitoring LULC changes over time from 1972 to 2022 provides critical insights into the spatial and temporal dynamics of human activities and natural processes affecting the landscape. By analyzing patterns of LULC change, such as urban expansion, vegetation, and water fluctuations, local planners and environmental mangers can identify areas that have undergone significant transformation or are at risk of environmental degradation. Our findings enable the detection of hotspots of land degradation or regions experiencing rapid urban growth, thereby helping to prioritize areas that require immediate environmental protection, restoration efforts, or more stringent land use regulations. Moreover, understanding these patterns supports informed decision making for sustainable land management and helps in planning controlled urban development, ensuring that future growth minimizes negative ecological impacts while supporting socioeconomic development goals.

Land use changes, including urban expansion, significantly impact biodiversity in the Wadi Fatimah and Wadi Uranah basins. The widespread and ongoing urbanization in these areas is adversely affecting local ecosystems and species diversity. In regions undergoing rapid urban growth, it is critically important to strike a balance between sustainable development and biodiversity conservation. To guide such efforts, ecologists have proposed the following two main strategies: land sparing and land sharing [63]. Land sparing involves setting aside large, contiguous areas exclusively for conservation (large vegetation patches), while concentrating urban development in separate zones [64]. In contrast, land sharing incorporates conservation within urban areas by distributing smaller, dispersed vegetation patches throughout the developed landscape [64]. A study by Soga et al. [65] in Tokyo, Japan, suggested that land sharing is more suitable for areas with lower levels of urbanization, while land sparing is more effective in regions with higher urban intensity. Meanwhile, a study by Ibáñez-Álamo et al. [66], conducted in nine European cities, concluded that no single planning strategy is universally applicable. Regardless of the approach, it is essential to account for the unique land characteristics of desert biomes to effectively reduce biodiversity loss in these arid environments.

5.5. Image Classification and Validation

The classification results indicate that the SVM technique effectively delineated LULC maps for both the Wadi Fatimah and Wadi Uranah basins. Among various machine learning approaches, SVM is recognized for its strong mathematical foundation and high classification accuracy [67]. Several studies have evaluated the performances of different classifiers for land cover mapping. For example, Dabija, et al. [68] found that SVM with a radial basis function (RBF) kernel outperformed other classifiers in identifying land cover features. Xie and Niculescu [69] compared the performances of three machine learning algorithms—SVM, Random Forest (RF), and Convolutional Neural Network (CNN)—for

monitoring LULC changes. While all algorithms demonstrated a satisfactory classification accuracy, CNN showed a superior performance compared to SVM and RF. In this study, only the SVM classifier was employed to monitor LULC changes in the Wadi Fatimah and Wadi Uranah basins from 1972 to 2022. The results demonstrated that SVM is a robust and reliable classification algorithm for these arid environments. However, future studies are recommended to compare the performances of other machine learning classifiers in the study area to potentially improve accuracy and classification outcomes.

Since satellite image classification can introduce errors or uncertainties, validating classification results is essential to ensure the accuracy of the resulting thematic LULC maps [70]. The accurate assessment of classification performance requires high-quality reference data against which the classified maps can be compared [71]. However, obtaining reference samples from field observations is particularly challenging for historical satellite imagery. As a result, visual image interpretation is often used to generate reference samples for accuracy assessment [71]. Although this method may introduce some degree of uncertainty, it remains a practical and widely accepted approach for validating classification results [72]. Accuracy can be further improved by increasing the number and effectiveness of training samples used to validate and represent various land cover features.

5.6. Advantages and Limitations

The results of this study demonstrate that remote sensing data (e.g., Landsat imagery) effectively capture the spatial extent of LULC features, enabling robust change detection over time. Remote sensing offers a powerful and cost-effective tool for monitoring LULC dynamics, providing consistent, large-scale, and repeatable observations essential for spatial and temporal analysis. This advantage is further strengthened by the integration of landscape metrics. Combining remote sensing data with landscape metrics enhances the ability to quantify and interpret spatial patterns and structural changes in LULC. This integration supports detailed assessments of landscape fragmentation, connectivity, and temporal dynamics, contributing to more informed environmental evaluation and land management decisions. The analysis conducted in this research highlights the value of remote sensing for monitoring and quantifying LULC changes over the past five decades in a rapidly developing region of Saudi Arabia.

Although LULC changes can be effectively spatially quantified using remote sensing data, the underlying processes driving these changes are often complex and cannot be fully explained by satellite observations alone. While remote sensing provides essential spatial and temporal information, it primarily captures surface-level changes without accounting for the socioeconomic and biophysical factors that influence landscape transformations. To achieve a more comprehensive understanding of LULC dynamics, it is crucial to incorporate ancillary variables such as elevation, slope, population density, income levels, and urban development policies. These additional datasets can provide contextual insights that enhance the interpretation of observed changes and support the identification of underlying causes, trends, and potential environmental and socioeconomic impacts. An integrated approach that combines remote sensing with environmental and socioeconomic variables offers a more holistic framework for analyzing landscape dynamics and supports more informed land use planning and sustainable development strategies. Nevertheless, the primary objective of this study was to investigate the spatiotemporal patterns of LULC changes in the Wadi Fatimah and Wadi Uranah basins over the past five decades. This type of descriptive analysis is fundamental for characterizing the spatial and temporal dimensions of landscape changes and serves as a critical foundation for assessing impacts, informing policy, and guiding effective land management decisions.

While Landsat imagery is well-suited for long-term LULC observations, differences in the spatial resolution of Landsat sensors can introduce inconsistencies when comparing images over time. The TM, ETM+, and OLI sensors all offer a spatial resolution of 30 m, whereas the older MSS sensor provides imagery at a coarser resolution of 60 m. To enable consistent time series analysis, a resampling technique is required to match the spatial resolution across all images. However, although resampling adjusts the pixel size to a common resolution, it may degrade the quality of the original data. This can negatively impact classification accuracy and introduce uncertainties. Acknowledging these limitations is crucial for developing more robust techniques that optimize the use of historical Landsat data for long-term environmental monitoring.

6. Conclusions

LULC changes and their consequences have become an area of interest in current scientific research on environmental change. This research aimed to quantify LULC change patterns using multi-temporal satellite images and landscape metrics in the upper basins of the Wadi Fatimah and Wadi Uranah fluvial systems in Makkah Province. The analysis of classification images and landscape metrics showed significant LULC changes in urban areas from 1972 through to 2022. The incorporation of both remote sensing and landscape metrics was effective, enabling the detection of changes along with the measurement of landscape ecology. This approach helped to clarify the spatial patterns of LULC changes in the study area.

The study identified two phases of urban spatial expansion, with the first phase occurring after 1972 and the second after 2000. While spatial urban expansion was limited and gradual during the first phase, it became large and extensive in the second phase. This approach to analyzing spatial urban expansion provides essential information to help local planners and decision makers ensure environmental sustainability and protect natural ecology.

This study offers key insights into the patterns of LULC changes in the Wadi Fatimah and Wadi Uranah basins over the past fifty years. Understanding these changes is essential for analyzing LULC trends and supporting planners and local authorities in Makkah in their decision-making processes. Additionally, measuring LULC changes is fundamental for various ecological and environmental research efforts.

Although the methods used in this study effectively identified the spatial distribution of LULC changes in both the Wadi Fatimah and Wadi Uranah basins, integrating socioeconomic variables such as population density and biophysical variables (e.g., elevation, and slope) into the analysis could provide deeper insights into the underlying causes of these spatial patterns. Understanding the driving forces behind LULC changes in each basin is crucial for improving planning strategies and promoting sustainable development. Furthermore, combining satellite data with LULC change models to project future scenarios could offer a more comprehensive understanding of the past, present, and potential future trajectories of LULC dynamics in the region. Such analyses would support the development of informed and sustainable policies aimed at mitigating future environmental changes.

Author Contributions: Conceptualization, A.F.A. and O.A.A.; methodology, A.F.A.; software, A.F.A.; validation, A.F.A. and O.A.A.; formal analysis, A.F.A.; investigation, A.F.A.; resources, O.A.A.; data curation, A.F.A.; writing—original draft preparation, A.F.A.; writing—review and editing, O.A.A.; visualization, A.F.A.; supervision, O.A.A.; project administration, A.F.A.; funding acquisition, A.F.A. All authors have read and agreed to the published version of the manuscript.

Funding: This research received no external funding.

Data Availability Statement: The data are available upon request.

Conflicts of Interest: The authors declare no conflicts of interest.

References

1. Gounaridis, D.; Chorianopoulos, I.; Symeonakis, E.; Koukoulas, S. A Random Forest-Cellular Automata modelling approach to explore future land use/cover change in Attica (Greece), under different socio-economic realities and scales. *Sci. Total Environ.* **2019**, *646*, 320–335. [CrossRef] [PubMed]
2. Zeng, L.; Yang, L.; Su, L.; Hu, H.; Feng, C. The impact of policies on land use and land cover changes in the Beijing–Tianjin–Hebei region in China. *Environ. Impact Assess. Rev.* **2025**, *110*, 107676. [CrossRef]
3. Keck, F.; Peller, T.; Alther, R.; Barouillet, C.; Blackman, R.; Capo, E.; Chonova, T.; Couton, M.; Fehlinger, L.; Kirschner, D.; et al. The global human impact on biodiversity. *Nature* **2025**, *641*, 395–400. [CrossRef]
4. Guan, D.; Li, H.; Inohae, T.; Su, W.; Nagaie, T.; Hokao, K. Modeling urban land use change by the integration of cellular automaton and Markov model. *Ecol. Model.* **2011**, *222*, 3761–3772. [CrossRef]
5. Lohwasser, J.; Bolognesi, T.; Schaffer, A. Impacts of population, affluence and urbanization on local air pollution and land transformation—A regional STIRPAT analysis for German districts. *Ecol. Econ.* **2025**, *227*, 108416. [CrossRef]
6. Kamwi, J.M.; Cho, M.A.; Kaetsch, C.; Manda, S.O.; Graz, F.P.; Chirwa, P.W. Assessing the spatial drivers of land use and land cover change in the protected and communal areas of the Zambezi Region, Namibia. *Land* **2018**, *7*, 131. [CrossRef]
7. Xu, G.; Chen, B. Generating a series of land covers by assimilating the existing land cover maps. *ISPRS J. Photogramm. Remote Sens.* **2019**, *147*, 206–214. [CrossRef]
8. Gómez, C.; White, J.C.; Wulder, M.A. Optical remotely sensed time series data for land cover classification: A review. *ISPRS J. Photogramm. Remote Sens.* **2016**, *116*, 55–72. [CrossRef]
9. Li, Y.; Chen, J.; Rao, Y. A practical sampling method for assessing accuracy of detected land cover/land use change: Theoretical analysis and simulation experiments. *ISPRS J. Photogramm. Remote Sens.* **2018**, *144*, 379–389. [CrossRef]
10. Zhang, C.; Sargent, I.; Pan, X.; Li, H.; Gardiner, A.; Hare, J.; Atkinson, P.M. Joint Deep Learning for land cover and land use classification. *Remote Sens. Environ.* **2019**, *221*, 173–187. [CrossRef]
11. Denize, J.; Hubert-Moy, L.; Betbeder, J.; Corgne, S.; Baudry, J.; Pottier, E. Evaluation of using sentinel-1 and-2 time-series to identify winter land use in agricultural landscapes. *Remote Sens.* **2018**, *11*, 37. [CrossRef]
12. Shih, H.; Stow, D.A.; Tsai, Y.H. Guidance on and comparison of machine learning classifiers for Landsat-based land cover and land use mapping. *Int. J. Remote Sens.* **2019**, *40*, 1248–1274. [CrossRef]
13. Alqurashi, A.F.; Kumar, L.; Sinha, P. Urban Land Cover Change Modelling Using Time-Series Satellite Images: A Case Study of Urban Growth in Five Cities of Saudi Arabia. *Remote Sens.* **2016**, *8*, 838. [CrossRef]
14. Ye, Z.; Yang, K.; Lin, Y.; Guo, S.; Sun, Y.; Chen, X.; Lai, R.; Zhang, H. A comparison between Pixel-based deep learning and Object-based image analysis (OBIA) for individual detection of cabbage plants based on UAV Visible-light images. *Comput. Electron. Agric.* **2023**, *209*, 107822. [CrossRef]
15. Bayazit, M.; Dönmez, C.; Berberoglu, S. Assessing the efficiency of pixel-based and object-based image classification using deep learning in an agricultural Mediterranean plain. *Environ. Monit. Assess.* **2025**, *197*, 155. [CrossRef]
16. Šímová, P.; Gdulová, K. Landscape indices behavior: A review of scale effects. *Appl. Geogr.* **2012**, *34*, 385–394. [CrossRef]
17. Zylshal; Sulma, S.; Yulianto, F.; Nugroho, J.; Sofan, P. A support vector machine object based image analysis approach on urban green space extraction using Pleiades-1A imagery. *Model. Earth Syst. Environ.* **2016**, *2*, 54. [CrossRef]
18. Tzotsos, A.; Argialas, D. Support vector machine classification for object-based image analysis. In *Object-Based Image Analysis*; Springer: Berlin/Heidelberg, Germany, 2008; pp. 663–677.
19. Liu, H.; Weng, Q. Landscape metrics for analysing urbanization-induced land use and land cover changes. *Geocarto Int.* **2013**, *28*, 582–593. [CrossRef]
20. Liu, T.; Yang, X. Monitoring land changes in an urban area using satellite imagery, GIS and landscape metrics. *Appl. Geogr.* **2015**, *56*, 42–54. [CrossRef]
21. O'Neill, R.V.; Krummel, J.R.; Gardner, R.H.; Sugihara, G.; Jackson, B.; DeAngelis, D.L.; Milne, B.T.; Turner, M.G.; Zygmunt, B.; Christensen, S.W.; et al. Indices of landscape pattern. *Landsc. Ecol.* **1988**, *1*, 153–162. [CrossRef]
22. McGarigal, K.; Romme, W.H.; Crist, M.; Roworth, E. Cumulative effects of roads and logging on landscape structure in the San Juan Mountains, Colorado (USA). *Landsc. Ecol.* **2001**, *16*, 327–349. [CrossRef]
23. McGarigal, K.; Marks, B.J. *Spatial Pattern Analysis Program for Quantifying Landscape Structure*; General Technical Report PNW-GTR-351; US Department of Agriculture, Forest Service, Pacific Northwest Research Station: Portland, OR, USA, 1995; pp. 1–122.
24. Sinha, P.; Kumar, L.; Reid, N. Rank-based methods for selection of landscape metrics for land cover pattern change detection. *Remote Sens.* **2016**, *8*, 107. [CrossRef]
25. Vincent, P. *Saudi Arabia: An Environmental Overview*; CRC Press: Boca Raton, FL, USA, 2008.
26. Alqurashi, A.F.; Kumar, L. Land Use and Land Cover Change Detection in the Saudi Arabian Desert Cities of Makkah and Al-Taif Using Satellite Data. *Adv. Remote Sens.* **2014**, *3*, 106–119. [CrossRef]

27. Rahman, M.T.; Aldosary, A.S.; Mortoja, M.G. Modeling Future Land Cover Changes and Their Effects on the Land Surface Temperatures in the Saudi Arabian Eastern Coastal City of Dammam. *Land* **2017**, *6*, 36. [CrossRef]
28. Alqurashi, A.F.; Kumar, L. Spatiotemporal patterns of urban change and associated environmental impacts in five Saudi Arabian cities: A case study using remote sensing data. *Habitat Int.* **2016**, *58*, 75–88. [CrossRef]
29. Anisurrahman, M.; Alshuwaikhat, H.M. Determining Sustainability Assessment Indicators for the Holy City of Makkah, Saudi Arabia. *Arab. J. Sci. Eng.* **2019**, *44*, 5165–5178. [CrossRef]
30. Ascoura, I.E. Impact of pilgrimage (Hajj) on the urban growth of the Mecca. *J. Educ. Soc. Res.* **2013**, *3*, 255–263. [CrossRef]
31. Alqurashi, A.F.; Kumar, L. An assessment of the impact of urbanization and land use changes in the fast-growing cities of Saudi Arabia. *Geocarto Int.* **2017**, *34*, 78–97. [CrossRef]
32. Jelil Niang, A.; Hermas, E.; Alharbi, O.; Al-Shaery, A. Monitoring landscape changes and spatial urban expansion using multi-source remote sensing imagery in Al-Aziziyah Valley, Makkah, KSA. *Egypt. J. Remote Sens. Space Sci.* **2020**, *23*, 89–96. [CrossRef]
33. Alqurashi, A.F. Quantification of Urban Patterns and Processes through Space and Time Using Remote Sensing Data: A Comparative Study between Three Saudi Arabian Cities. *Sustainability* **2021**, *13*, 12615. [CrossRef]
34. Subyani, A.M. Hydrologic behavior and flood probability for selected arid basins in Makkah area, western Saudi Arabia. *Arab. J. Geosci.* **2011**, *4*, 817–824. [CrossRef]
35. Al-Hathloul, S.; Mughal, M.A. Urban growth management-the Saudi experience. *Habitat Int.* **2004**, *28*, 609–623. [CrossRef]
36. Alqurashi, A.F.; Kumar, L.; Al-Ghamdi, K.A. Spatiotemporal Modeling of Urban Growth Predictions Based on Driving Force Factors in Five Saudi Arabian Cities. *ISPRS Int. J. Geo-Inf.* **2016**, *5*, 139. [CrossRef]
37. Appiah-Twum, M.; Xu, W.; Sunkari, E. Mapping Lithology with Hybrid Attention Mechanism–Long Short-Term Memory: A Hybrid Neural Network Approach Using Remote Sensing and Geophysical Data. *Remote Sens.* **2024**, *16*, 4613. [CrossRef]
38. Benz, U.C.; Hofmann, P.; Willhauck, G.; Lingenfelder, I.; Heynen, M. Multi-resolution, object-oriented fuzzy analysis of remote sensing data for GIS-ready information. *ISPRS J. Photogramm. Remote Sens.* **2004**, *58*, 239–258. [CrossRef]
39. Drăguţ, L.; Tiede, D.; Levick, S.R. ESP: A tool to estimate scale parameter for multiresolution image segmentation of remotely sensed data. *Int. J. Geogr. Inf. Sci.* **2010**, *24*, 859–871. [CrossRef]
40. Li, Q.; Wang, C.; Zhang, B.; Lu, L. Object-based crop classification with Landsat-MODIS enhanced time-series data. *Remote Sens.* **2015**, *7*, 16091–16107. [CrossRef]
41. Gleason, C.J.; Im, J. Forest biomass estimation from airborne LiDAR data using machine learning approaches. *Remote Sens. Environ.* **2012**, *125*, 80–91. [CrossRef]
42. Xu, L.; Li, J.; Brenning, A. A comparative study of different classification techniques for marine oil spill identification using RADARSAT-1 imagery. *Remote Sens. Environ.* **2014**, *141*, 14–23. [CrossRef]
43. Thanh Noi, P.; Kappas, M. Comparison of random forest, k-nearest neighbor, and support vector machine classifiers for land cover classification using Sentinel-2 imagery. *Sensors* **2017**, *18*, 18. [CrossRef]
44. Mountrakis, G.; Im, J.; Ogole, C. Support vector machines in remote sensing: A review. *ISPRS J. Photogramm. Remote Sens.* **2011**, *66*, 247–259. [CrossRef]
45. Ishida, H.; Oishi, Y.; Morita, K.; Moriwaki, K.; Nakajima, T.Y. Development of a support vector machine based cloud detection method for MODIS with the adjustability to various conditions. *Remote Sens. Environ.* **2018**, *205*, 390–407. [CrossRef]
46. Jung, M. LecoS-A QGIS Plugin for Automated Landscape Ecology Analysis. *PeerJ Prepr.* **2013**, *1*, e116v2.
47. Sertel, E.; Topaloğlu, R.H.; Şallı, B.; Yay Algan, I.; Aksu, G.A. Comparison of Landscape Metrics for Three Different Level Land Cover/Land Use Maps. *ISPRS Int. J. Geo-Inf.* **2018**, *7*, 408. [CrossRef]
48. Seto, K.C.; Fragkias, M. Quantifying Spatiotemporal Patterns of Urban Land-use Change in Four Cities of China with Time Series Landscape Metrics. *Landsc. Ecol.* **2005**, *20*, 871–888. [CrossRef]
49. Dietzel, C.; Herold, M.; Hemphill, J.J.; Clarke, K.C. Spatio-temporal dynamics in California's Central Valley: Empirical links to urban theory. *Int. J. Geogr. Inf. Sci.* **2005**, *19*, 175–195. [CrossRef]
50. Nolasco, M.; Balzarini, M. Assessment of temporal aggregation of Sentinel-2 images on seasonal land cover mapping and its impact on landscape metrics. *Environ. Monit. Assess.* **2025**, *197*, 142. [CrossRef]
51. McGarigal, K.; Cushman, S.A.; Neel, M.; Ene, E. FRAGSTATS: Spatial Pattern Analysis Program for Categorical Maps. Computer Software Program Produced by the Authors at the University of Massachusetts, Amherst. 2002. Available online: https://www.fragstats.org (accessed on 13 November 2024).
52. Zhao, Y.; Tomita, M.; Hara, K.; Fujihara, M.; Yang, Y.; Da, L. Effects of topography on status and changes in land-cover patterns, Chongqing City, China. *Landsc. Ecol. Eng.* **2014**, *10*, 125–135. [CrossRef]
53. Li, X.; Zhou, W.; Ouyang, Z. Forty years of urban expansion in Beijing: What is the relative importance of physical, socioeconomic, and neighborhood factors? *Appl. Geogr.* **2013**, *38*, 1–10. [CrossRef]
54. Bindajam, A.A.; Mallick, J. Impact of the Spatial Configuration of Streets Networks on Urban Growth: A Case Study of Abha City, Saudi Arabia. *Sustainability* **2020**, *12*, 1856. [CrossRef]

55. Al-Huqail, A.A.; Al-Harbi, H.F.; Alowaifeer, A.M.; El-Sheikh, M.A.; Assaeed, A.M.; Alsaleem, T.S.; Kassem, H.S.; Azab, O.M.; Dar, B.A.; Malik, J.A.; et al. Correlation between aboveground vegetation composition and soil seed bank of Raudhat desert habitat: A case study of Raudhat Alkhafs, Saudi Arabia. *BMC Plant Biol.* **2025**, *25*, 136. [CrossRef]
56. Liu, W.; Wu, J.; Xu, F.; Mu, D.; Zhang, P. Modeling the effects of land use/land cover changes on river runoff using SWAT models: A case study of the Danjiang River source area, China. *Environ. Res.* **2024**, *242*, 117810. [CrossRef]
57. Banjara, M.; Bhusal, A.; Ghimire, A.B.; Kalra, A. Impact of Land Use and Land Cover Change on Hydrological Processes in Urban Watersheds: Analysis and Forecasting for Flood Risk Management. *Geosciences* **2024**, *14*, 40. [CrossRef]
58. Wang, N.; Chen, X.; Zhang, Y.; Pang, J.; Long, Z.; Chen, Y.; Zhang, Z. Integrated effects of land use and land cover change on carbon metabolism: Based on ecological network analysis. *Environ. Impact Assess. Rev.* **2024**, *104*, 107320. [CrossRef]
59. Hussain, S.; Karuppannan, S. Land use/land cover changes and their impact on land surface temperature using remote sensing technique in district Khanewal, Punjab Pakistan. *Geol. Ecol. Landsc.* **2023**, *7*, 46–58. [CrossRef]
60. Pande, C.B.; Diwate, P.; Orimoloye, I.R.; Sidek, L.M.; Pratap, M.A.; Moharir, K.N.; Pal, S.C.; Alshehri, F.; Tolche, A.D. Impact of land use/land cover changes on evapotranspiration and model accuracy using Google Earth engine and classification and regression tree modeling. *Geomat. Nat. Hazards Risk* **2024**, *15*, 2290350. [CrossRef]
61. Ahmadi, H.; Popalzai, A.; Bekbotayeva, A.; Omarova, G.; Assubayeva, S.; Arshamov, Y.; Pekkan, E. Assessing the Impacts of Landuse-Landcover (LULC) Dynamics on Groundwater Depletion in Kabul, Afghanistan's Capital (2000–2022): A Geospatial Technology-Driven Investigation. *Geosciences* **2024**, *14*, 132. [CrossRef]
62. Soltani, A.; Azizi, P.; Javadpoor, M.; Allan, A.; Bagheri, B. Determining and Quantifying Urban Sprawl Drivers: A Delphi-DANP Approach. *Land* **2025**, *14*, 311. [CrossRef]
63. Green, R.E.; Cornell, S.J.; Scharlemann, J.P.W.; Balmford, A. Farming and the Fate of Wild Nature. *Science* **2005**, *307*, 550–555. [CrossRef] [PubMed]
64. Fischer, J.; Abson, D.J.; Butsic, V.; Chappell, M.J.; Ekroos, J.; Hanspach, J.; Kuemmerle, T.; Smith, H.G.; von Wehrden, H. Land Sparing Versus Land Sharing: Moving Forward. *Conserv. Lett.* **2014**, *7*, 149–157. [CrossRef]
65. Soga, M.; Yamaura, Y.; Koike, S.; Gaston, K.J. Land sharing vs. land sparing: Does the compact city reconcile urban development and biodiversity conservation? *J. Appl. Ecol.* **2014**, *51*, 1378–1386. [CrossRef]
66. Ibáñez-Álamo, J.D.; Morelli, F.; Benedetti, Y.; Rubio, E.; Jokimäki, J.; Pérez-Contreras, T.; Sprau, P.; Suhonen, J.; Tryjanowski, P.; Kaisanlahti-Jokimäki, M.; et al. Biodiversity within the city: Effects of land sharing and land sparing urban development on avian diversity. *Sci. Total Environ.* **2020**, *707*, 135477. [CrossRef]
67. Chandra, M.A.; Bedi, S.S. Survey on SVM and their application in imageclassification. *Int. J. Inf. Technol.* **2021**, *13*, 1–11. [CrossRef]
68. Dabija, A.; Kluczek, M.; Zagajewski, B.; Raczko, E.; Kycko, M.; Al-Sulttani, A.H.; Tardà, A.; Pineda, L.; Corbera, J. Comparison of Support Vector Machines and Random Forests for Corine Land Cover Mapping. *Remote Sens.* **2021**, *13*, 777. [CrossRef]
69. Xie, G.; Niculescu, S. Mapping and Monitoring of Land Cover/Land Use (LCLU) Changes in the Crozon Peninsula (Brittany, France) from 2007 to 2018 by Machine Learning Algorithms (Support Vector Machine, Random Forest, and Convolutional Neural Network) and by Post-classification Comparison (PCC). *Remote Sens.* **2021**, *13*, 3899.
70. Congalton, R.G.; Green, K. *Assessing the Accuracy of Remotely Sensed Data: Principles and Practices*, 3rd ed.; CRC Press: Boca Raton, FL, USA, 2019.
71. Zhao, Y.; Gong, P.; Yu, L.; Hu, L.; Li, X.; Li, C.; Zhang, H.; Zheng, Y.; Wang, J.; Zhao, Y.; et al. Towards a common validation sample set for global land-cover mapping. *Int. J. Remote Sens.* **2014**, *35*, 4795–4814. [CrossRef]
72. Li, C.; Wang, J.; Wang, L.; Hu, L.; Gong, P. Comparison of Classification Algorithms and Training Sample Sizes in Urban Land Classification with Landsat Thematic Mapper Imagery. *Remote Sens.* **2014**, *6*, 964–983. [CrossRef]

Disclaimer/Publisher's Note: The statements, opinions and data contained in all publications are solely those of the individual author(s) and contributor(s) and not of MDPI and/or the editor(s). MDPI and/or the editor(s) disclaim responsibility for any injury to people or property resulting from any ideas, methods, instructions or products referred to in the content.